

Effects of urban density on carbon dioxide exchanges: observations of dense urban, suburban and woodland areas of southern England

Article

Published Version

Creative Commons: Attribution 3.0 (CC-BY)

Open Access

Ward, H. C., Kotthaus, S., Grimmond, C. S. B. ORCID: <https://orcid.org/0000-0002-3166-9415>, Bjorkegren, A., Wilkinson, M., Morrison, W. T. J., Evans, J. G., Morison, J. I. L. and Iamarino, M. (2015) Effects of urban density on carbon dioxide exchanges: observations of dense urban, suburban and woodland areas of southern England. *Environmental Pollution*, 198. pp. 186-200. ISSN 0269-7491 doi: 10.1016/j.envpol.2014.12.031 Available at <https://centaur.reading.ac.uk/39050/>

It is advisable to refer to the publisher's version if you intend to cite from the work. See [Guidance on citing](#).

To link to this article DOI: <http://dx.doi.org/10.1016/j.envpol.2014.12.031>

Publisher: Elsevier

copyright holders. Terms and conditions for use of this material are defined in the [End User Agreement](#).

www.reading.ac.uk/centaur

CentAUR

Central Archive at the University of Reading

Reading's research outputs online



Effects of urban density on carbon dioxide exchanges: Observations of dense urban, suburban and woodland areas of southern England



H.C. Ward ^{a, c, *}, S. Kotthaus ^{a, b}, C.S.B. Grimmond ^a, A. Borgegren ^b, M. Wilkinson ^d,
W.T.J. Morrison ^a, J.G. Evans ^c, J.I.L. Morison ^d, M. Iamarino ^e

^a Department of Meteorology, University of Reading, Reading, RG6 6BB, UK

^b Department of Geography, King's College London, London, WC2R 2LS, UK

^c Centre for Ecology and Hydrology, Wallingford, Oxfordshire, OX10 8BB, UK

^d Forest Research, Centre for Forestry and Climate Change, Alice Holt Lodge, Farnham, Surrey, GU10 4LH, UK

^e Scuola di Ingegneria, Università degli Studi della Basilicata, 85100, Potenza, Italy

ARTICLE INFO

Article history:

Received 27 May 2014

Received in revised form

12 October 2014

Accepted 26 December 2014

Available online

Keywords:

Carbon emissions

Emissions inventory

Human impact

Land use change

Net ecosystem exchange

ABSTRACT

Anthropogenic and biogenic controls on the surface–atmosphere exchange of CO₂ are explored for three different environments. Similarities are seen between suburban and woodland sites during summer, when photosynthesis and respiration determine the diurnal pattern of the CO₂ flux. In winter, emissions from human activities dominate urban and suburban fluxes; building emissions increase during cold weather, while traffic is a major component of CO₂ emissions all year round. Observed CO₂ fluxes reflect diurnal traffic patterns (busy throughout the day (urban); rush-hour peaks (suburban)) and vary between working days and non-working days, except at the woodland site. Suburban vegetation offsets some anthropogenic emissions, but 24-h CO₂ fluxes are usually positive even during summer. Observations are compared to estimated emissions from simple models and inventories. Annual CO₂ exchanges are significantly different between sites, demonstrating the impacts of increasing urban density (and decreasing vegetation fraction) on the CO₂ flux to the atmosphere.

© 2015 The Authors. Published by Elsevier Ltd. This is an open access article under the CC BY license (<http://creativecommons.org/licenses/by/4.0/>).

1. Introduction

Carbon dioxide concentrations continue to increase globally, reaching 400 ppm on a daily basis at Mauna Loa in 2013 (The Keeling Curve, 2014). Over 70% of global greenhouse gas emissions are from urban areas (IEA, 2012). While a large number of studies have documented the seasonal dynamics of carbon fluxes of vegetated ecosystems (e.g. Schmid et al., 2000; Baldocchi et al., 2001; Aubinet et al., 2012), comparable measurements from urban areas remain relatively limited (see reviews by Velasco and Roth, 2010; Grimmond and Christen, 2012; Christen, 2014; Weissert et al., 2014). The earliest measurements in cities began in the mid-1990s (Grimmond et al., 2002; Nemitz et al., 2002), yet only very recently have multi-year urban fluxes been published (Pawlak et al., 2010; Bergeron and Strachan, 2011; Crawford et al., 2011; Järvi et al., 2012; Liu et al., 2012; Peters and McFadden,

2012). Thus understanding of CO₂ exchanges based on direct observations in regions with large urban fluxes is limited. Instead, estimates of emissions are mostly based on fuel consumption inventories, but these tend to have coarse spatial and temporal resolution and do not include biogenic processes such as photosynthetic uptake by urban vegetation (Järvi et al., 2012; Crawford and Christen, 2014). However, to explore the potential impacts of urban planning schemes and policy decisions, or to make predictions about future climates, improved understanding of processes relevant to the urban carbon balance is required. Pataki et al. (2011) highlight the need for more rigorous evaluation of urban greening schemes, which should include both positive and negative impacts on the ecosystem as a whole, realistic cost-benefit analyses and consideration of site-specific and species-dependent behaviour.

Per unit area, annual CO₂ exchanges measured in urban areas greatly exceed those from nearby natural ecosystems: average annual CO₂ release in Helsinki is forty times larger than the uptake by a nearby wetland and eight times larger than the uptake by a boreal forest (Järvi et al., 2012). In highly-vegetated Baltimore,

* Corresponding author. Department of Meteorology, University of Reading, Reading, RG6 6BB, UK.

E-mail address: h.c.ward@reading.ac.uk (H.C. Ward).

however, net CO₂ release is similar in magnitude to the net uptake of nearby forests (Crawford et al., 2011). Few campaigns have quantified CO₂ exchanges for different urban densities concurrently. Coutts et al. (2007) presented fluxes from two suburban sites in Melbourne, and Bergeron and Strachan (2011) compared fluxes from urban, suburban and agricultural sites in Montreal. Measurements of CO₂ concentration across urban-to-rural gradients in the US include the work of Strong et al. (2011) in Salt Lake Valley and Briber et al. (2013) in Boston. Given the apparent inability of vegetation to assimilate large enough quantities of CO₂ to offset emissions (Pataki et al., 2011; Weissert et al., 2014), quantifying the effect of human behaviour on CO₂ exchange becomes an even more critical area for research. Approaches include long-term observational campaigns which encompass policy changes, for example Song and Wang (2012) assessed the impact of traffic reduction due to the Beijing Olympics in 2008, and combining measurements and models to better inform the attribution of measured CO₂ emissions to various human activities such as building energy use, transport and metabolism (e.g. Christen et al., 2011; Strong et al., 2011).

The objective of this study is to relate observed CO₂ exchanges to physical processes, through consideration of meteorological conditions and surface characteristics. Direct eddy covariance measurements of CO₂ fluxes from three very different land uses (urban, suburban and woodland) over the same period are compared. The sites are located within one of the most densely populated regions of Europe: southern England. This region, which includes London, has been extensively modified by human activities in both rural and urban areas. Atmospheric controls are considered first, by comparing the meteorology observed at each site. After demonstrating the similarity in climatic conditions, links between CO₂ flux and surface characteristics (e.g. land cover, urban density) are explored.

2. Materials and methods

2.1. Description of sites

In this paper measurements undertaken at three sites 70–100 km apart and at approximately the same latitude in southern England (Table 1, Fig. 1) are compared. These are a dense urban environment in central London (U); a predominantly residential suburban site in Swindon (S); and a deciduous oak woodland at the Alice Holt Research site (W). Additional details are provided elsewhere (London (Kotthaus and Grimmond, 2012;

2014a,b); Swindon (Ward et al., 2013); Alice Holt (Wilkinson et al., 2012)).

Across the sites there is a gradient of impervious to pervious land cover, with London having 81% of the plan area covered by roads and buildings, Swindon 49% and Alice Holt effectively 0% (Table 1). The heights of the roughness elements (i.e. buildings and trees) are similar in London and Alice Holt (>20 m) but smaller in Swindon (≈6 m). There is very little vegetation at the central London site; trees are mainly London plane (*Platanus hispanica*) and grass lawns are mainly confined to small public gardens. In Swindon, grass is the predominant surface cover and grows alongside roads as well as in residential gardens, recreational areas and on undeveloped land. Trees comprise a range of species but are mainly deciduous. At Alice Holt the predominant tree species is oak (*Quercus robur*) with hazel (*Corylus avellana*) and hawthorn (*Crataegus monogyna*) making up the understorey (Wilkinson et al., 2012). The above and below ground tree biomass is estimated to be 13.4 kg C m⁻² (excluding shrubs and ground flora, based on 2009 data) and the mean peak leaf area index is 5.9 m² m⁻² (1999–2010 data).

2.2. Instrumentation and data processing

Net fluxes of CO₂ between the surface and atmosphere were obtained for 30-min intervals using the eddy covariance (EC) technique at each site. The micrometeorological sign convention is used, i.e. negative flux indicates CO₂ uptake by the surface and positive flux indicates CO₂ release. The instrumental setup is summarised in Table 2. Equipment was mounted on towers (a square-section tower at Alice Holt, lattice towers in London and a pneumatic mast in Swindon) to ensure that measurements were made well above the mean height of the roughness elements (z_H) and above the roughness sub-layer ($>2 z_H$ for U and S; $> 1.3 z_H$ for W, Tables 1 and 2). Sites were carefully selected to ensure the measurements are representative of the local environment. Although the source areas vary with meteorological conditions, footprint models indicate that the majority of the flux usually originates from within a few hundred metres (approximately 200–400 m) of the towers; at night these distances increase (to around 600–700 m) as instability decreases. The variation in land cover around each tower is far smaller than the difference in land cover between the three sites. Full characterisation is provided in the individual site papers.

Raw data from the sonic and gas analyser were processed using LiCOR's EddyPro software (S, W) or ECPACK (van Dijk et al., 2004) (U). The quality control procedures applied were selected based on the requirements of each site, dependent on their different characteristics (see Kotthaus and Grimmond, 2012, Ward et al., 2013 and Wilkinson et al., 2012 for details). This was judged to be the most appropriate methodology, rather than attempting to apply a single set of tests across all sites which may not be suitable for each environment. All sites were subject to the following standard procedures: adjustment for the lag time between sonic anemometer and gas analyser; correction of sonic temperature for humidity; correction for spectral losses. The planar fit coordinate transformation was applied to the London data; double coordinate rotation was used for Swindon and Alice Holt. Data from all sites were despiked and subjected to physically-reasonable threshold checks and data were removed during times of instrument malfunction. In London the influence of micro-scale building emissions was removed from the local-scale fluxes using an algorithm based on the statistical characteristics of turbulent events (Kotthaus and Grimmond, 2012); this procedure is not required at the less urbanised sites. No friction velocity (u_*) threshold was used to reject CO₂ fluxes at the suburban or urban site because the rough

Table 1

Site characteristics (values are those given in the respective publications; surface cover is calculated at U for the average footprint climatology (Kotthaus and Grimmond, 2014b), at S for 500 m around the tower (Ward et al., 2013) and at W for the woodland area (Wilkinson et al., 2012)). z_H is the average building or tree height; z_d zero plane displacement height; z_0 roughness length.

	London (U)	Swindon (S)	Alice Holt (W)
Location	51°30' N 0°07' W	51°35' N 1°48' W	51°09' N 0°51' W
Classification	Urban	Suburban	Woodland
Description	High density central business district	Low-rise residential	Deciduous oak plantation
z_H [m]	22.0	5.5	21.0
z_d [m]	14.2	3.5	15.3
z_0 [m]	1.9	0.5	2.2
Surface cover [%]			
Impervious	43	33	0
Buildings	38	16	0
Vegetation (trees)	5 (2)	44 (9)	98 (97)
Open water	14	0	0.5
Bare soil	0	6	1.5

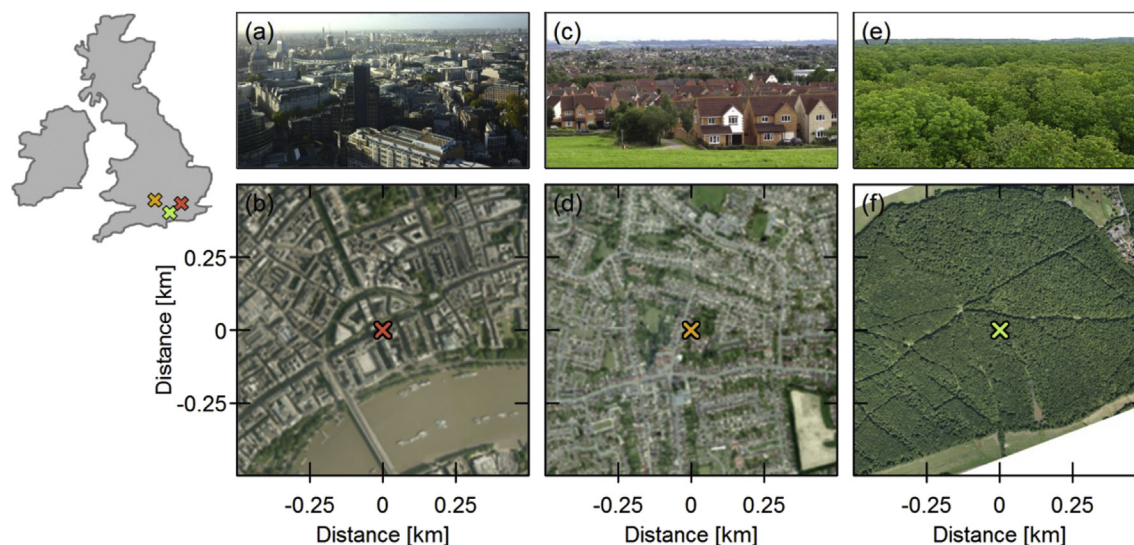


Fig. 1. Photographs and aerial images of the (a–b) London, (c–d) Swindon and (e–f) Alice Holt sites with the positions of the eddy covariance towers indicated (crosses) (2009 ©GeoPerspectives: b, d).

nature of these surfaces and anthropogenic energy emissions enhance mixing, resulting in fewer stable periods (Christen and Vogt, 2004) which means that thresholds developed for rural environments are not useful (Bergeron and Strachan, 2011; Crawford et al., 2011; Liu et al., 2012). At Alice Holt, inspection of plots of night-time fluxes against u^* suggested a threshold of 0.15 m s^{-1} . This is similar to the average threshold value derived for the site between 1999 and 2010 by Wilkinson et al. (2012) and is within the range found for woodland sites (e.g. $0.1\text{--}0.5 \text{ m s}^{-1}$, Papale et al. (2006)). CO_2 fluxes were therefore excluded for $u^* < 0.15 \text{ m s}^{-1}$ at W. In this study no corrections were made for CO_2 storage below the EC instruments at any of the sites (accounting for storage would alter the fluxes by $<0.5\%$ at W, and the correction for urban areas is estimated to be only a few percent (Crawford and Christen, 2012)).

The period analysed comprises January 2011 to April 2013, with all three sites operational from May 2011. Gaps in the data occurred due to a variety of operational reasons (e.g. low power, instrument failure) but the overall data availability is reasonably good. Out of the maximum possible 40848 30-min periods, after quality control CO_2 fluxes were available for analysis 77.0%, 57.1% and 70.3% of the time at London, Swindon and Alice Holt, respectively. Available data were relatively evenly spread between day and night, although less so at Alice Holt where the u^* filter excluded a larger proportion of night-time data (76.8% of data are available during the day compared to 63.9% at night).

For calculation of annual totals, CO_2 fluxes for 2011 and 2012 were gap-filled using monthly median diurnal cycles (e.g. Järvi et al., 2012). Two sets of median diurnal cycles were calculated

for each site, one for working days and the other for non-working days (weekends and holidays), for each of the 28 months. These were used to fill gaps in the datasets based on month, day of week and time of day for each site. As data collection in Swindon did not start until May 2011, the period January–April 2011 was filled using the mean of the 2012 and 2013 diurnal cycles for each month (January–April) considering working days and non-working days separately. Implications of this procedure are discussed below (Section 4.3).

Other variables measured (Table 2) include photosynthetically active radiation (PAR) at the U and W sites. Comparison of measured PAR and total incoming solar radiation (K_t) for these sites revealed a high degree of correlation ($r^2 = 0.99$) with constants of proportionality (PAR/K_t , both in W m^{-2}) of 0.38 and 0.42 at U and W, respectively. Gaps in measured PAR were filled using these relations with K_t where possible. For S, PAR was modelled as a proportion (0.40) of incoming shortwave radiation.

2.3. Estimating anthropogenic emissions

Carbon emissions for the central London site were estimated with the GreaterQF model (Iamarino et al., 2012) after updating gas (domestic and non-domestic) and other fuel consumption data with 2011–2012 data (DECC, 2013a), and residential and daytime population with 2011 census data (ONS, 2011). Traffic emissions were adjusted for the study period according to the trends in annual totals provided for the relevant central London boroughs (DECC, 2013b). CO_2 emissions from fuel combustion were

Table 2
Instrumentation details (model and measurement height, h) for the three sites. The London site tower was moved to another part of the building (from 'KSS' to 'KSSW') in March 2012.

	London (U)		Swindon (S)		Alice Holt (W)	
	Model	h [m]	Model	h [m]	Model	h [m]
Sonic anemometer	CSAT3, Campbell Scientific	48.9 (KSS) 50.3 (KSSW)	R3, Gill Instruments	12.5	Solent R2, R3 Gill Instruments	28.0
Infrared gas analyser	Li-7500, LiCOR Biosciences	48.9 (KSS) 50.3 (KSSW)	Li-7500, LiCOR Biosciences	12.5	Li-7000, LiCOR Biosciences	28.0
Radiometer	CNR1/CNR4, Kipp & Zonen	48.9 (KSS) 50.3 (KSSW)	NR01, Hukseflux	10.1	CM3, Kipp & Zonen	27.0
PAR sensor	PAR Quantum, Skye Instruments	37.0	—	—	BF3, Delta-T Devices	27.0
Weather station	WXT510/520, Vaisala	48.9 (KSS) 50.3 (KSSW)	WXT510/520, Vaisala	10.6	HMP50, Vaisala	27.0

calculated by applying conversion factors (NGVA) to heat emissions, as provided by GreaterQF, while CO₂ emissions from human metabolism were estimated following Koerner and Klopatek (2002). Emissions were modelled for the borough of Westminster, which contains the majority of the EC footprint.

Estimates of anthropogenic carbon emissions were made for the Swindon site using inventories of domestic energy use, vehicle use and population density (see Appendix A of Ward et al. (2013) for details). Quarterly domestic natural gas consumption statistics (DECC, 2013a) were used to estimate CO₂ emissions due to building energy use (combustion of other fuels was neglected) with sub-daily variability modelled based on Hamilton et al. (2009). The total distance travelled by motor vehicles in Swindon (DfT, 2013) was adjusted for the proportion of road in the study area. Equal weight of traffic across all roads (Ichinose et al., 1999), a fixed fuel economy (Sailor and Lu, 2004) and fixed emission factors (Moriwaki and Kanda, 2004) were assumed in the absence of more detailed data specific to Swindon. Temporal variation was modelled using typical daily and monthly profiles (DfT, 2011). CO₂ release from human metabolism was estimated using daytime and nighttime population density (ONS, 2011) following the method of Bergeron and Strachan (2011).

3. Variability in meteorological conditions

Due to their proximity, the three sites can be expected to experience similar climatic conditions and weather patterns. Southern England has a temperate maritime climate (cool summers, mild winters, cloudy, wet and changeable weather). According to the Met Office (2014a,b), normal (1981–2010) annual rainfall for this region is 782 mm and mean air temperature (T_{air}) is 10.3 °C. In both 2011 and 2012, rainfall was well below normal at the start of the year. Whilst 2011 remained drier than normal, the rest of 2012 was very wet with above average rainfall (April–December). The summers of 2011 and 2012 were generally cloudy, although there were some warm, dry and sunny spells in late May, July and September 2012 (Figs. 2 and 3). Winter 2011/12 was warmer than average but a cold period brought snowfall in February 2012. Winter 2012/13 was cool and temperatures remained low throughout spring, with March 2013 being much colder than normal.

Regional similarities in weather patterns are evident in the data collected at the London, Swindon and Alice Holt sites (Fig. 2). Although instrumental differences have not been accounted for, the mean daily air temperatures at measurement height follow each other closely ($r^2 > 0.94$). The slightly warmer air temperatures at U compared to S and then W are as expected. Mean daily temperatures are 15.94, 15.29 and 14.85 °C in summer and 5.34, 4.99 and

4.82 °C in winter at U, S and W, respectively. Fig. 2 also shows that the patterns in relative humidity (RH) are similar between sites, and again show the expected variation with land use (highest humidity at the woodland site and lowest in the city centre).

When T_{air} and RH are combined to give vapour pressure deficit (VPD), periods with high VPD are easily identifiable at all three sites simultaneously (Fig. 3, shading). These warm, dry spells occur when the incoming shortwave radiation is high across the region and skies are near clear (Fig. 3, bars). Diurnal and seasonal behaviour in VPD and PAR are important controls on photosynthesis rates (e.g. Schmid et al., 2000; Flanagan et al., 2002). Comparing across the sites, K_d decreases as the density of urbanisation increases. Although the time series in Fig. 3 are very similar, the colouring reveals that higher transmissivity tends to occur at W. These findings are as expected, as there is evidence of reduced solar radiation receipt in central London (Ryder and Toumi, 2011). Modelled bulk transmissivity was determined as the fraction of observed K_d relative to the top of atmosphere K_d (calculated using the solaR R package (Perpiñán, 2012) and a solar constant of 1367 W m⁻² (Peixoto and Oort, 1992)). The mean bulk transmissivity for the study period was 0.372, 0.382 and 0.415 at U, S and W, respectively. Overall, it can be concluded that the three sites experience generally similar weather conditions and therefore any differences in CO₂ exchanges should be related to land-surface controls.

4. Results and discussion

4.1. CO₂ flux comparison between sites

There are clear contrasts in both the magnitude and temporal variability of the observed carbon fluxes (F_c) in London, Swindon and Alice Holt (Fig. 4). At the forested Alice Holt site, the annual cycle is dominated by the balance between photosynthesis and respiration (Fig. 4c). Net uptake in the daytime by the understorey is evident early in the year (Wilkinson et al., 2012), followed by a sudden increase in net uptake which coincides with leaf-out of the oak canopy (Mizunuma et al., 2013). During the night and in winter, the forest acts as a small source of CO₂. The largest emissions occur during summer nights (5–6 μmol m⁻² s⁻¹) when ecosystem respiration rates are largest because the vegetation is in leaf and metabolically more active, and temperatures are warm (Figs. 4c and 5c). The behaviour observed at Alice Holt is typical for deciduous forests generally (Falge et al., 2002; Baldocchi et al., 2005) and for other deciduous forest areas in this region (Thomas et al., 2011).

In contrast, central London is a major source of CO₂ all year round, with larger emissions during winter than summer (Fig. 4a). Emissions are 10–30 μmol m⁻² s⁻¹ larger during the day than the night (Fig. 5a) and the shape of the diurnal pattern in the CO₂ flux

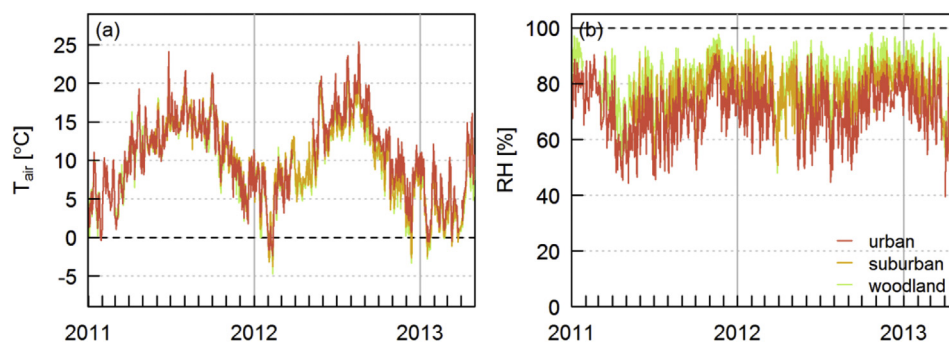


Fig. 2. Comparison of meteorological conditions at the three sites (daily mean values) showing variability within the study period and consistency across the region for (a) air temperature and (b) relative humidity. Missing data have not been gap-filled.

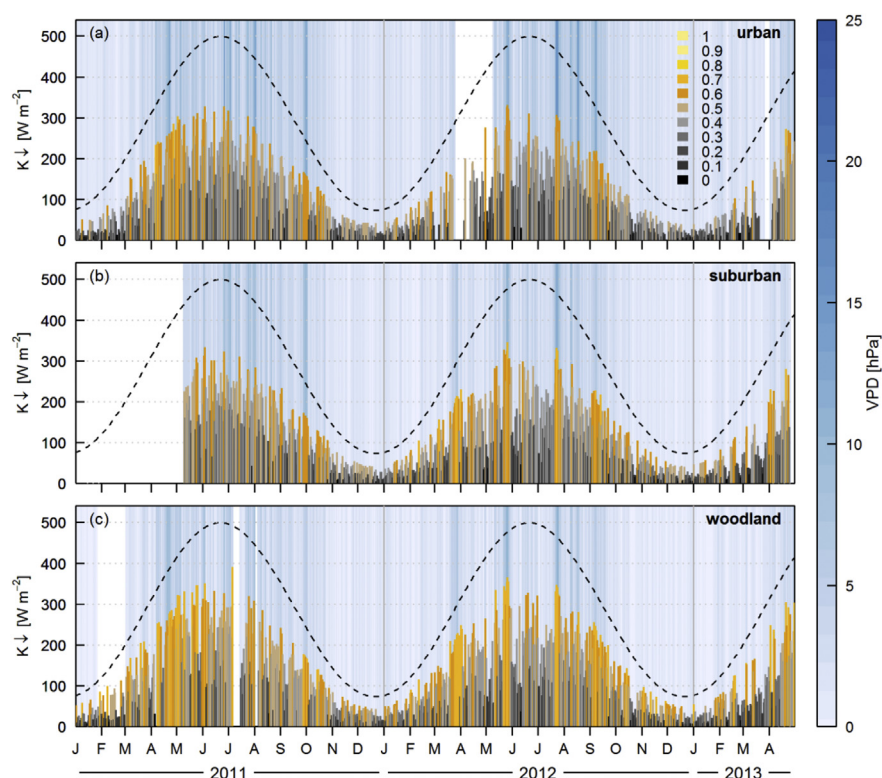


Fig. 3. Mean daily measured incoming solar radiation (K_{\downarrow} , bars) coloured according to modelled bulk transmissivity. Top of atmosphere K_{\downarrow} is shown by the dashed line. Mean daily vapour pressure deficit (VPD in blue) is indicated by the background shading (right hand legend). White areas are due to missing data. (For interpretation of the references to colour in this figure legend, the reader is referred to the web version of this article.)

does not differ considerably with season, being slightly asymmetrical and tending to remain higher in the evening approaching midnight compared to the early hours of the morning (Fig. 6). This is in accordance with expected typical patterns of human behaviour

and similar to those documented in Tokyo (Moriwaki and Kanda, 2004) or Marseille (Grimmond et al., 2004), for example. In densely built-up areas both the abundance of sources and sustained daytime activity (e.g. from traffic, human metabolism and

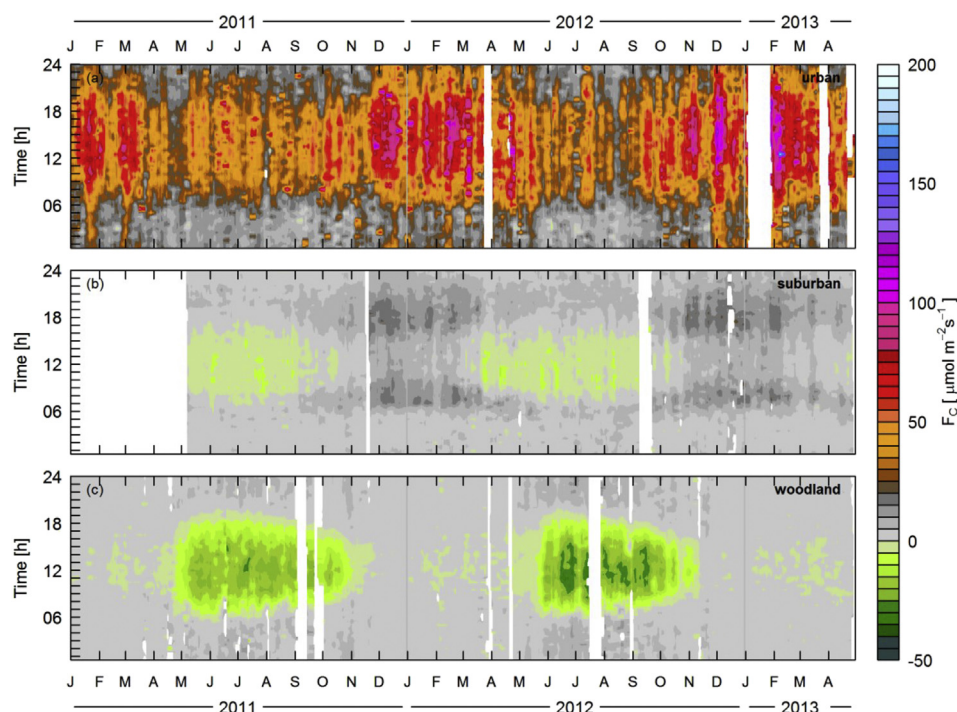


Fig. 4. Carbon dioxide fluxes by time of day (y-axis) and date (x-axis) at the three sites calculated as 7-day running means.

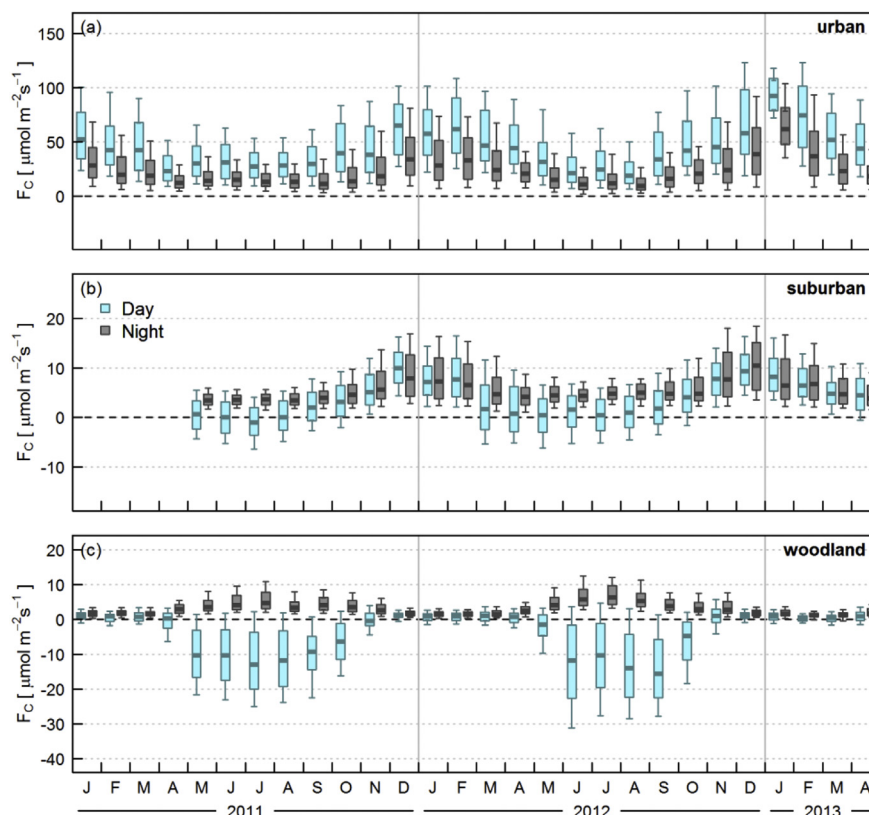


Fig. 5. Daytime and night time 30-min carbon dioxide fluxes by month. Boxes enclose the interquartile range (IQR); medians are indicated by thick horizontal lines; whiskers enclose the 10th to 90th percentiles. Note different scales on the y-axes between the sites.

commercial building use) cause emissions to stay high throughout the day (e.g. Helfter et al., 2011; Iamarino et al., 2012; Lietzke and Vogt, 2013). Average daytime values peak at about $35 \mu\text{mol m}^{-2} \text{s}^{-1}$ in summer and $80 \mu\text{mol m}^{-2} \text{s}^{-1}$ in winter. Note the availability of CO_2 data at U is very low for January 2013 (4.8%, all occurring on weekdays, Fig. 4a). The monthly values for January 2013 in Figs. 5a and 6 are therefore very likely overestimates of the true CO_2 fluxes.

Suburban Swindon, having a mixture of vegetation cover plus built areas, has fluxes that respond to both biogenic and anthropogenic controls. As for London, Swindon's emissions are largest in

winter (Fig. 4b), when there is increased fuel combustion for building heating and vegetation is largely dormant. During the growing season photosynthetic uptake is greatest in the middle of the day, associated with maximal PAR. The pattern of daytime CO_2 fluxes is similar to W (Fig. 6). However, during winter the diurnal pattern of F_C is markedly different: two clear peaks are observed which coincide with road traffic and building heating demand during the morning and evening rush hours (Ward et al., 2013). The role of human activities resulting in differences in F_C between U and S is evident. In U the emissions remain high throughout the day-time, reflecting the intensity of activities. In low density residential

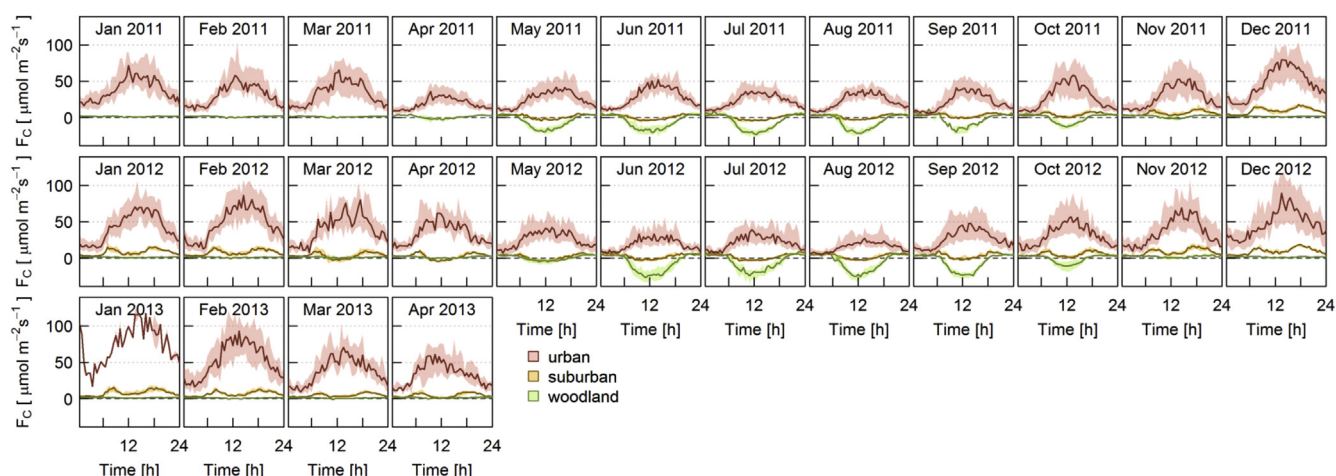


Fig. 6. Monthly median diurnal cycles and interquartile ranges (shaded) of 30-min carbon dioxide fluxes for January 2011 to April 2013 for the three sites.

areas, such as Swindon, rush-hour peaks are more typically observed, for example in Melbourne (Coutts et al., 2007), Montreal (Bergeron and Strachan, 2011), Helsinki (Järvi et al., 2012) and Mexico City (Velasco et al., 2013). Typical wintertime fluxes are approximately five times smaller at S ($9 \text{ g C m}^{-2} \text{ day}^{-1}$) than U ($50 \text{ g C m}^{-2} \text{ day}^{-1}$), whilst summertime fluxes are roughly ten times smaller at S ($2 \text{ g C m}^{-2} \text{ day}^{-1}$) than U ($22 \text{ g C m}^{-2} \text{ day}^{-1}$).

Uptake of CO_2 in towns and cities is often masked by anthropogenic emissions, partly as the proportion of land covered by vegetation tends to be considerably lower (e.g. 44% at S) than in the surrounding countryside or before development. Despite the significant amount of vegetation at S, the net daily (24-h) flux is usually positive. Nevertheless, the potential of urban vegetation to reduce the overall release of CO_2 into the atmosphere is evident in the Swindon data (Fig. 6). From spring until autumn, F_C is negative during the middle of the day and 24-h emissions are kept low ($\approx 2 \text{ g C m}^{-2} \text{ d}^{-1}$). Photosynthesis continues into the autumn, but increased emissions from heating at S mean that uptake is no longer seen in the middle of the day (compare fluxes at S and W during October and early November, Fig. 4).

As there are no anthropogenic emissions at the woodland site, the photosynthetic uptake is a strong signal in the observed CO_2 flux (\approx net ecosystem exchange (NEE)). The ecosystem respiration (R_{eco}) at this site is around $5\text{--}10 \text{ } \mu\text{mol m}^{-2} \text{ s}^{-1}$ during summer daytimes (Wilkinson et al., 2012), so gross primary production (GPP) may typically be $40 \text{ } \mu\text{mol m}^{-2} \text{ s}^{-1}$ around midday during the peak of the growing season. At W, the diurnal range in the CO_2 flux is small in winter ($F_C \approx 0\text{--}3 \text{ } \mu\text{mol m}^{-2} \text{ s}^{-1}$) but there is still a small yet discernible reduction in CO_2 release during the middle of the day (Fig. 4c). These estimates of R_{eco} are consistent with long-term averages at this site and other similar sites (Wilkinson et al., 2012). Chamber measurements made at W in 2007–2010 (Heinemeyer et al., 2012) indicated soil CO_2 effluxes are equal to about half of R_{eco} .

At all times the CO_2 release from the U site exceeds that from S and W. The CO_2 fluxes are most comparable during the early hours of the morning in summer (e.g. June, July and August 2012) at around $3\text{--}10 \text{ } \mu\text{mol m}^{-2} \text{ s}^{-1}$; these represent amongst the smallest emissions from U and largest emissions from W. The spread of observed values is greatest at U, small and stays the same all year round at S, while W data are much more variable in summer.

Despite the additional sources of CO_2 at S compared to at W, the observed fluxes were lower at S during daytimes in spring 2012 (March and April), and similar around midday during May 2012 and April 2013 (Figs. 4b–c and 6). This may be due to the slightly warmer temperatures within urban areas which cause leaf development to occur earlier, but also reflects the large soil decomposition and tree respiration rates in woodland environments. Phenological differences of extended growing season in urban environments have been observed in a number of areas (e.g. Imhoff et al., 2004; Zhang et al., 2004). Unfortunately no S data are available before May 2011, so it is not possible to extend this comparison over more years. There is also some species dependency: photosynthetic activity occurs in the shrub layer at W from late February (Wilkinson et al., 2012, 1999–2010 data) but the tree canopy does not develop until late April–May; most of the vegetation around the residential S site is grass that can begin photosynthesising early in the year (Hiller et al., 2011). Although both sites have a small proportion of evergreen vegetation (other than grass), it is unlikely to be a significant contribution at either site.

Inter-annual differences in the CO_2 fluxes are mainly attributable to variations in the weather. Largely warm and sunny conditions in April and early May 2011 (Fig. 3) promoted development of vegetation and led to a rapid increase in the rate of photosynthesis.

In 2012, a dry, sunny spell in March was followed by a very wet and dull April, which resulted in rapid leaf-out of deciduous vegetation at the end of May (Fig. 3). In early 2013, positive F_C observed across all sites is attributed to the cold start to the year (Fig. 2) suppressing vegetation growth and generating a greater demand for building heating and thus increased CO_2 emissions.

4.2. Relation to biophysical processes and anthropogenic activities

To assess the roles of biophysical processes and anthropogenic activities at the three very different sites, relations with explanatory variables are investigated here. Whilst Alice Holt essentially has no emissions from human activity, the tiny amount of vegetation around the London site is insufficient to be detectable compared to the strong anthropogenic signal. Swindon lies between the two with fluxes that relate to a mixture of controls. Analysis over relatively long time series (28 months) also permits exploration of seasonal trends and inter-annual variability.

4.2.1. Photosynthetically active radiation

During the growing season photosynthetic uptake by vegetation exhibits a clear dependence on the amount of PAR received by leaves. As PAR increases, observed F_C at both S and W decreases. When vegetation is fully leafed-out, data closely follow the expected functional dependence (Fig. 7). Seasonally, the F_C –PAR relation varies: as vegetation approaches senescence the relation between PAR and rate of CO_2 uptake decreases as the leaf area changes at both W and S (not shown). Naturally, the woodland ecosystem has the strongest dependence on PAR as the footprint is completely vegetated and during summer daytimes photosynthesis constitutes the main component of F_C . As the largest PAR values are approached, the rate of CO_2 uptake decreases and the curves level off as the light saturation threshold for photosynthesis is reached. At times with high PAR (i.e. sunny weather, typically warm with a high VPD, Fig. 3), when there is limited water available, plants may reduce transpiration rates to conserve water. Levelling off of the light response curve, or even a reduction in CO_2 uptake at high PAR, may also indicate stomatal closure. Separating morning and

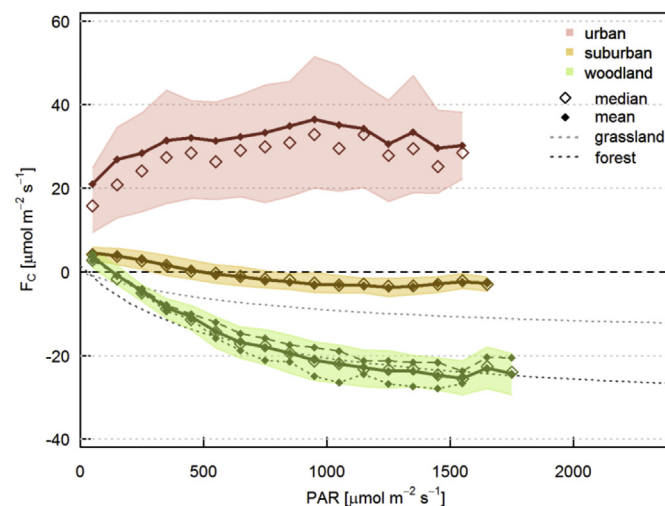


Fig. 7. Relation between carbon dioxide fluxes and photosynthetically active radiation (PAR) for summer daytimes (June–August 2011 and 2012), i.e. when leaves are fully out. PAR data are used to group the fluxes into bins of $100 \text{ } \mu\text{mol m}^{-2} \text{ s}^{-1}$, with only those bins containing >25 data points shown. The interquartile range for each site is shaded. Dashed lines are empirical models for temperate grassland (Flanagan et al., 2002) and broadleaf forest (Schmid et al., 2000). For the woodland site, the relations for 2011 (dashed line) and 2012 (dotted line) are also shown separately.

afternoon data reveals some diurnal hysteresis, with slightly higher uptake at moderate to large PAR in the morning compared to the afternoon at S and W. At W the uptake in 2011 (drier than average, dashed line in Fig. 7) is lower than in 2012 (a very wet summer, dotted line) across mid-to-high PAR values. There is also some asymmetry in the diurnal cycles of F_C in late summer 2011 (Fig. 6), which may be due to limited water availability. However, note that there are large data gaps in September 2011 for W (Fig. 4).

At U there is no clear relation with PAR. The spread of the data is much greater and mean values are higher than the medians as a result of some large F_C values and a slight positive skew (more so in summer 2012, Fig. 5a). The observed increase in F_C at low PAR values is probably related to the coincident increase (decrease) in anthropogenic activities following sunrise (before sunset). The lack of evidence for photosynthetic uptake in central London indicates that the role of vegetation is negligible at this densely urbanised site.

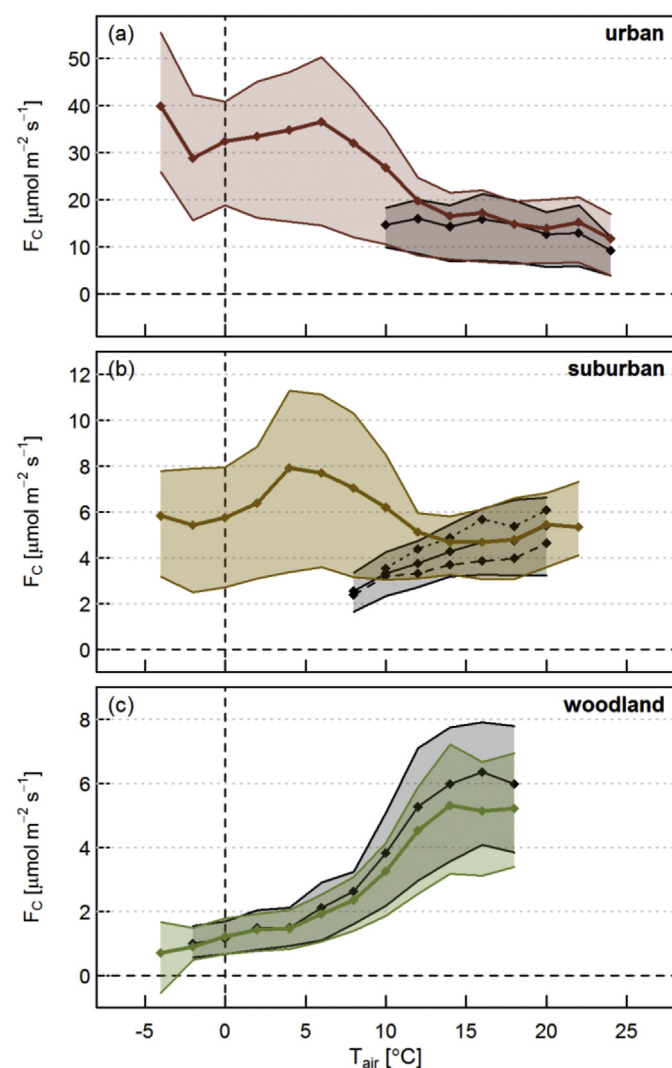


Fig. 8. Night time carbon dioxide fluxes versus air temperature (30 min) in bins of 2 °C. Only bins containing >25 data points are plotted and the interquartile range for each site is shaded. Night time data are classified based on solar angle with the additional criterion that $PAR < 10 \mu\text{mol m}^{-2} \text{s}^{-1}$. Black curves indicate subsets of the data: (a) summertime only (June–August 2011 and June–August 2012); (b) summertime only (as above); (c) the period April 2012–April 2013. In (b) summertime (June–August) data for 2011 (dashed line) and 2012 (dotted line) are also shown separately.

4.2.2. Temperature

In natural environments, the nocturnal CO_2 flux is equated to ecosystem respiration. At W the expected exponential increase in ecosystem respiration with air temperature (e.g. Lloyd and Taylor, 1994; Schmid et al., 2000) is observed across the seasons (Fig. 8c). The variability increases with temperature and the CO_2 emissions level off above about 15 °C. This levelling-off may be caused by the grouping of data at different periods in the seasonal cycle, variability in soil moisture conditions or the changing relation between soil temperature and air temperature. Respiration rates are higher when soil conditions are wet at warmer temperatures, presumably due to higher decomposition rates, as indicated by the subset April 2012–April 2013 (a very wet period, Section 3).

During summer nights at S, when CO_2 emissions from traffic and building heating are minimal, F_C also shows an increase with T_{air} (subset, Fig. 8b), suggesting a contribution from ecosystem respiration. Again, emissions are larger during summer 2012 (dotted line) than during summer 2011 (dashed line), particularly for warm temperatures. Anthropogenic emissions dominate at cooler temperatures in response to increased heating demand. The coolest period occurred in February 2012 and included snowfall (Section 3). The rate of increase of F_C with decreasing T_{air} is greater at U than at S due to the difference in urban density. At U, R_{eco} (excluding human respiration) is a very small contributor to the total carbon emissions. Thus, an exponential dependence of R_{eco} on T_{air} is not seen, even in summer. Instead F_C decreases with increasing T_{air} and the relation levels off for the warmest temperatures (Fig. 8a).

At urbanised sites, monthly total carbon emissions are often negatively correlated with air temperature (e.g. Liu et al., 2012). Fig. 9 combines the effects of seasonal variation in vegetation activity and demand for building heating with temperature (assuming that traffic load is independent of temperature). At U a decrease in emissions with increasing temperature is seen for all months, as well as for winter and summer separately. The gradient ($-1.95 \mu\text{mol m}^{-2} \text{s}^{-1} \text{°C}^{-1}$) is larger in magnitude than the value given for Beijing ($-0.34 \mu\text{mol m}^{-2} \text{s}^{-1} \text{°C}^{-1}$ (Liu et al., 2012)), reflecting the greater seasonal variability and larger contribution of building activities to the total emissions at the London site compared to the Beijing site. As U is much more densely built, the

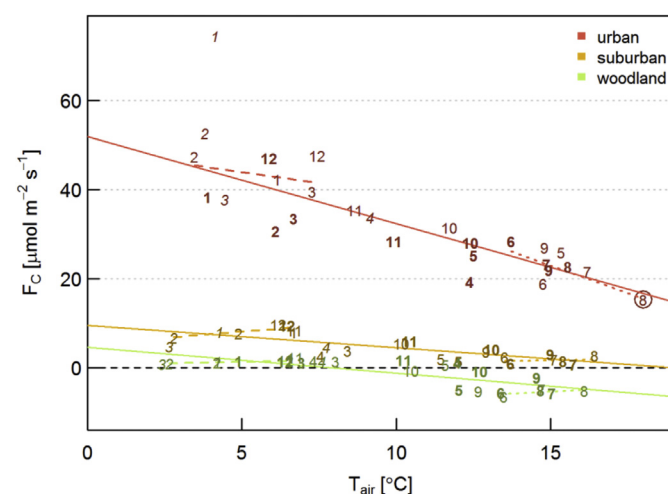


Fig. 9. Monthly mean carbon dioxide fluxes versus monthly mean temperatures. Numbers indicate months (1–12), with years **2011**, 2012 and 2013 in **bold**, roman and *italic*, respectively. Linear regressions for all months (solid lines), winter (DJF, dashed lines) and summer (JJA, dotted lines) are shown. The outlier for London is January 2013 and has been left out of the regressions for London due to low data availability (see Section 4.1). Alice Holt in February 2011 and London in April 2012 are not plotted due to lack of T_{air} data.

total emissions are also greater than in Beijing (15% vegetation fraction, P_V). Building-scale F_C is estimated to reach around $60 \mu\text{mol m}^{-2} \text{s}^{-1}$ in the morning hours (November 2009–June 2011) on average (Kotthaus and Grimmond, 2012). Emissions at the warmest temperatures are associated with traffic (assuming traffic does not vary seasonally) and metabolism, plus gas combustion for non-heating purposes. The London Olympics occurred during the warmest month, August 2012 (circled in Fig. 9), when central London traffic was less and more people used public transport (Tfl, 2012). Thus a more typical estimate associated with the slightly cooler summer months may be around $20 \mu\text{mol m}^{-2} \text{s}^{-1}$.

An overall trend of reduced emissions with warmer temperatures is seen for S, with a shallower gradient than for U. However, when winter and summer are considered separately at S, an increase in F_C with temperature is observed, possibly associated with increased respiration rates (Fig. 8b). Similar relations are seen for W, but the woodland site goes from being a source of CO_2 to a sink of CO_2 with increasing temperature (i.e. with season), whereas Swindon is always a net source of CO_2 on a monthly basis.

4.2.3. Day of week

The major impact of anthropogenic activities on the carbon fluxes is apparent when data are separated into working days and non-working days, i.e. weekends and holidays (Fig. 10). Over a long enough study period there is no reason for weather conditions or biogenic processes to differ substantially between working and non-working days. Thus, as expected, CO_2 fluxes from the woodland site do not show any significant systematic difference between these two subsets.

For the suburban site, however, F_C tends to be larger on working days compared to non-working days (Fig. 10). This is particularly

evident in winter when F_C is dominated by anthropogenic controls. The two ‘rush-hour’ peaks seen in the morning and evening are more pronounced on working days, while the diurnal pattern on non-working days is flatter with a reduced morning peak and a tendency for increased emissions during the middle of the day. These differences closely resemble patterns of human behaviour and energy consumption (e.g. Sailor, 2011). In winter, when vegetation is dormant, trends in observed F_C are modelled reasonably well by the estimated anthropogenic emissions, although the modelled emissions overestimate the observations. Emissions from traffic tend to show little seasonal variation, while emissions from building heating vary from month to month (due to temperature). Reduced building emissions are partly responsible for lower F_C observed in summer, but at this time of year photosynthesis dominates the shape of the diurnal cycle. Emissions from human metabolism are a small contribution ($\sim 1 \mu\text{mol m}^{-2} \text{s}^{-1}$) to total F_C .

For the London site, emissions are mostly determined by energy use in buildings, the majority of which is non-domestic gas combustion according to inventory data (DECC, 2013a). Emissions are considerably higher on working days than on non-working days all year round (by about $15\text{--}30 \mu\text{mol m}^{-2} \text{s}^{-1}$ at midday), with the largest fluxes usually occurring in the middle of the day. This is typical for the area, which is strongly service-oriented and has a large daytime population made up almost entirely of non-residents. Model results for the borough of Westminster (area 22.2 km^2) are presented here. Most of the EC source area is located within this borough, which has a resident population density of less than $10,000 \text{ persons km}^{-2}$ compared to a workday population density of $31,000 \text{ persons km}^{-2}$ (ONS, 2011). However, the total daytime population density (including tourists) is even higher, estimated at $46,000 \text{ persons km}^{-2}$ (GLA, 2013). For such densely

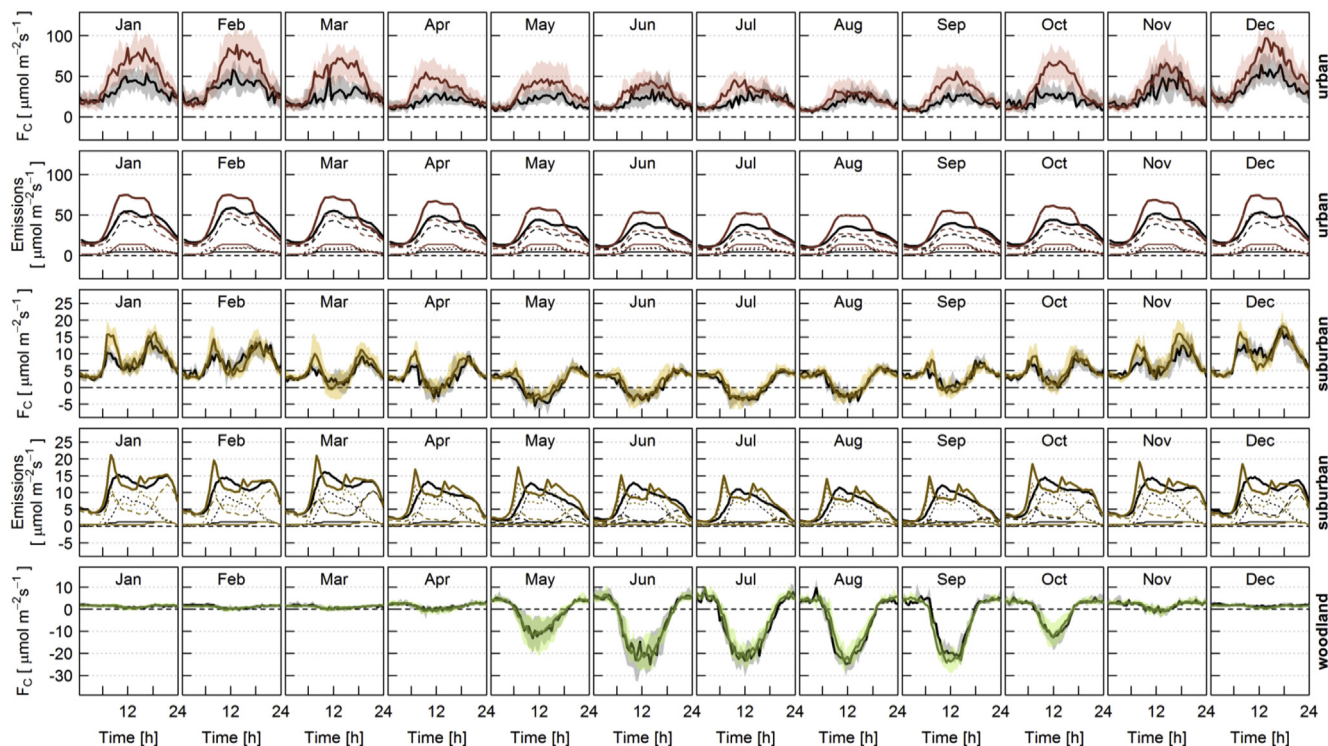


Fig. 10. Monthly median diurnal cycles and interquartile ranges (shaded) of the carbon dioxide flux for the three sites, separated into working days (colours) and non-working days (black). For London and Swindon, estimated anthropogenic emissions from building heating (dashed lines), traffic (dotted lines) and human metabolism (thin solid lines), and building heating, traffic and human metabolism combined (thick solid lines) are also shown (see text for details). Note London emissions are modelled for the borough of Westminster. Data from different years (2011–2013) have been combined by month here. (For interpretation of the references to colour in this figure legend, the reader is referred to the web version of this article.)

populated areas CO₂ emissions from human metabolism are a significant contribution to the total emissions, particularly during the middle of working days. The model assumes that the daytime population applies for times between 1000 and 1600, which is probably an oversimplification. In reality, people arrive earlier and leave later for work, while others may travel into the area in the evening. This difference may explain why the observed diurnal cycles are more peaked than the modelled diurnal cycles. The GreaterQF model does not account for seasonal variation in population density, although the daytime population is generally lower in summer coinciding with the holiday season for workers and students. As seen in Swindon, the traffic load at U is fairly steady all year round. The lowest emissions are associated with non-working days during summer. Vehicular emissions are estimated to contribute an average of 6.7/5.2 $\mu\text{mol m}^{-2} \text{s}^{-1}$ on working/non-working days to F_c ; building emissions are more significant at 23.7/22.6 $\mu\text{mol m}^{-2} \text{s}^{-1}$.

Overall, the GreaterQF model captures the shape of the diurnal cycle in F_c and differences between working days and non-working days reasonably well, in particular the fluxes on non-working days remaining high late into the evening. The model estimates for the borough of Westminster are slightly lower than the observations at U in winter and higher in summer. At smaller scales, GreaterQF emission estimates became very spatially variable, dominated by variation in non-domestic gas consumption. Emission estimates for some areas were more than twice the size of the observations at U. Such spatial contrast raises the question of whether energy use inventories are an appropriate method to estimate carbon fluxes at these scales. The location of individual buildings, roads or neighbourhoods with respect to the boundaries used for reporting energy use, traffic and population can have a major impact on the corresponding emissions estimated for that area. Validation would require far more detailed information than is available at present, both spatially and temporally. Considering the land cover at the London site in comparison with Westminster borough, we would expect traffic emissions to contribute to the observations at a greater extent than suggested by the model estimates in Fig. 10.

4.3. Annual totals and inter-annual variability

Cumulative carbon fluxes indicating net carbon uptake or release (Fig. 11) were obtained by gap-filling with monthly median

diurnal cycles (Section 2.2). Annual totals for the two complete years studied (2011/2012) are 12.08/13.36, 1.62/1.87 and $-0.46/-0.37 \text{ kg C m}^{-2} \text{ yr}^{-1}$ for U, S and W, respectively. (Note, as S began operating from May 2011 earlier data are all gap-filled.) Mean annual totals are: 12.72, 1.75 and $-0.42 \text{ kg C m}^{-2} \text{ yr}^{-1}$ for U, S and W, respectively (based on 2011 and 2012 data). The amount of carbon released at U and S was greater (by 10–15%) in 2012 compared to 2011 and the carbon uptake at W was smaller (by about 20%). Higher emissions in 2012 at U and S likely result from larger heating demand: cold weather including snowfall in February, a cool and wet April and a cooler autumn than normal. The timing of these differences between 2011 and 2012 can be seen in Fig. 11 (most clearly for U but the difference in autumn is also visible at S during October and November). F_c is noticeably smaller for August 2012 (16 $\text{g C m}^{-2} \text{ day}^{-1}$) than August 2011 (24 $\text{g C m}^{-2} \text{ day}^{-1}$) at U (see also Figs. 5a and 6), which may be partly due to reduced traffic during the London Olympics. It is not possible to quantify the impact of the Olympics on the CO₂ emissions with this dataset, as inter-annual variability can be driven by many factors, for instance August 2012 was also slightly warmer than 2011. But these results demonstrate the potential for human behaviour to affect emissions of CO₂, either indirectly via responses to synoptic weather conditions or due to entirely anthropogenic factors. Despite the later start to the growing season in 2012, the magnitude of daytime uptake at W was greater in 2012 than 2011, however, emissions from respiration were also larger in 2012 than 2011 (Fig. 4c). The annual carbon uptake at W during 2011 and 2012 is comparable to, but slightly smaller than, the 1999–2010 average of $-0.49 \text{ kg C m}^{-2} \text{ yr}^{-1}$ (Wilkinson et al., 2012) and well within the range observed in previous years: $-0.30 \text{ kg C m}^{-2} \text{ yr}^{-1}$ (2010, outbreak of defoliating caterpillars) to $-0.63 \text{ kg C m}^{-2} \text{ yr}^{-1}$ (2007, long growing season).

Järvi et al. (2012) compare various gap-filling techniques for an urban site in Helsinki, and find that the gap-filling method has only a small effect (<5%) on the estimates of annual CO₂ exchange. The continuous period January–April 2011 before measurements began at S needs to be considered differently (Section 2.2), because gap-filling using data from other years can introduce bias due to inter-annual variability of the fluxes. Temperatures in April 2012 were lower than April 2011 and February, March and April 2013 were cooler than the same months in 2011. Gap-filling the January–April 2011 data with the average of the diurnal cycles for

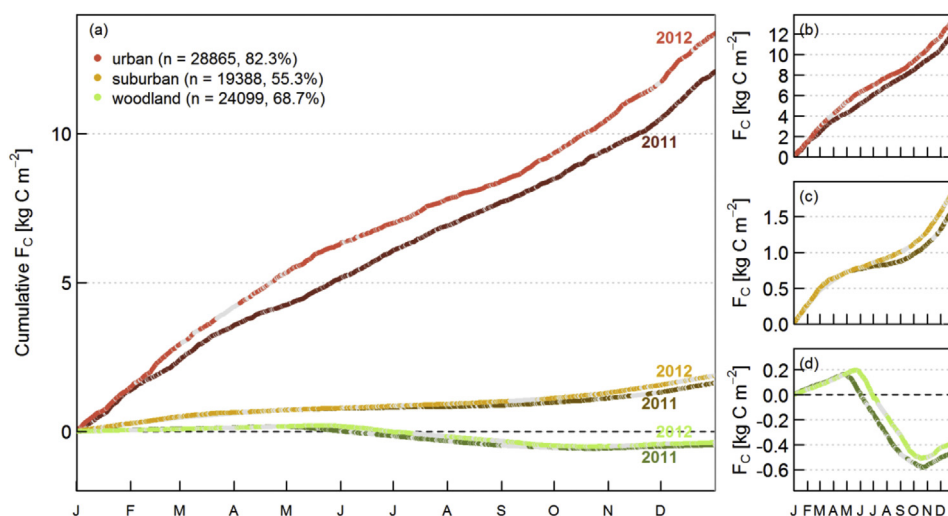


Fig. 11. Cumulative carbon flux over for the two complete years (2011, 2012) within the study period (a) for all sites together and (b–d) for each site individually. Grey points indicate data that have been gap-filled; the legend includes the proportion of data available for 2011–2012.

these months in 2012 and 2013 has therefore likely resulted in an overestimation of CO₂ release in 2011, as it is reasonable to expect the heating demand was lower in 2011 compared to in April 2012 and February–April 2013. The modelled emissions support this hypothesis: emissions from building heating are estimated to be 37% smaller in April 2011 than in April 2012 and 23% smaller in February–April 2011 than in February–April 2013. Additionally, the very cool and cloudy weather in April 2012 and cool temperatures in February–April 2013 are thought to have delayed photosynthetic uptake compared to spring 2011 (e.g. Fig. 5c), i.e. using the average of 2012 and 2013 data for spring 2011 likely underestimates uptake for this period. Again, this potential bias due to the gap-filling procedure would lead to an overestimation of CO₂ fluxes for Jan–Apr 2011. However, the estimated annual CO₂ release in 2011 is still smaller than for 2012. These year-to-year variations highlight the need for long-term measurements to evaluate emissions inventories.

On an annual basis, S emits four times more carbon per unit area than is absorbed at W, despite its relatively large proportion of vegetation cover. Per unit area, carbon emissions from U are thirty times larger than the uptake at the woodland site and seven times larger than emissions from the suburban site. These results can be considered in terms of the impact of land use change. In vegetated areas, deforestation followed by urbanisation can change a region from a net CO₂ sink to a net CO₂ source, which may emit ten or more times more CO₂ than was previously being taken up. The opposite effect may be observed in arid areas, however, where urbanisation can increase the amount of vegetation relative to the surroundings (Oke et al., 1989; Seto and Shepherd, 2009; Ramamurthy and Pardyjak, 2011).

Values from the National Atmospheric Emissions Inventory (NAEI, 2011) compare reasonably well with the results presented here, although, contrary to EC observations of the net CO₂ exchange, they do not account for biogenic processes such as ecosystem (including human) respiration and photosynthesis. Inventory data for the four 1 km × 1 km grid squares around the locations of each EC tower were considered. NAEI total emissions for the London site amounted to 13.00 kg C m⁻² yr⁻¹, almost all of which is due to non-industrial combustion (63%) and road use (34%). This value is similar to the observed F_C (12.72 kg C m⁻² yr⁻¹) and similar to the emission estimates from the GreaterQF model for Westminster (13.5 kg C m⁻² yr⁻¹, or 11.3 kg C m⁻² yr⁻¹ if human metabolism is not included). As discussed in Section 4.2.3, the traffic emissions from GreaterQF are thought to be an underestimate for the study site. The slightly lower emission estimates from GreaterQF may also be explained by land cover differences with the study site, as about 20% of Westminster borough is open green-

space (but the borough also includes some of the busiest streets in London).

In Swindon, non-industrial combustion and road use comprise nearly all (97%) of the total NAEI value of 1.92 kg C m⁻² yr⁻¹ (value calculated omitting one of the four grid squares with a large contribution from industrial processes which is outside the footprint of the EC system). The difference between the NAEI value and observed average annual total is 0.17 kg C m⁻² yr⁻¹, which is mainly attributed to the influence of vegetation on F_C (uptake of -0.12 kg C m⁻² yr⁻¹). The contribution of vegetation to F_C was approximated based on typical annual uptake from European grassland sites of 0.24 kg C m⁻² yr⁻¹ (Soussana et al., 2007) and uptake by trees of -0.42 kg C m⁻² yr⁻¹ (from the Alice Holt observations), scaled by the proportion of grass (36%) and tree (9%) cover in the study area.

The same comparison at Alice Holt offers little insight, as the NAEI estimates are based on processes which are largely unimportant at the woodland site. NAEI estimates vary around the EC tower, from 0.0027 kg C m⁻² yr⁻¹ for a grid square that is almost entirely vegetated with no roads or houses (note that this is most representative of the footprint of the EC system) to >0.3 kg C m⁻² yr⁻¹ when a main road is found within the grid square. The footprint of the EC system is mainly concentrated over the woodland (Wilkinson et al., 2012), so the emissions from these roads are not thought to impact F_C . However, it is remarkable that a few roads within a largely undeveloped and vegetated landscape result in modelled emissions of a similar order of magnitude to the woodland uptake.

A wide range of annual carbon fluxes from other urban areas around the world have been observed (Table 3). Both globally and across the three study sites in southern England, decreasing vegetation cover and increasing population density are associated with enhanced emissions (Fig. 12). Reduced vegetation cover coincides with an increased area of buildings and roads, and therefore greater associated emissions, as well as reduced capacity to take up CO₂. As the vegetation fraction of urban areas decreases, the building density increases for both the plan area and the height of buildings, and the population density increases. Hence F_C exponentially increases as vegetation cover decreases (Fig. 12a). The relation with population density appears to be more linear (Fig. 12b) and more scattered, as was also shown by Nordbo et al. (2012). There is considerable uncertainty associated with the population estimates. As already discussed, there is huge variation in the number of people in central London throughout the day, both spatially and temporally, and accurate quantification is challenging. Therefore this descriptor is often not reported consistently in the literature. Workday population densities according to the 2011 census are

Table 3
Annual observed carbon fluxes (F_C), vegetation cover (P_V) and population density (ρ_{pop}) from urban sites in the literature (with measurements for at least one year). Population densities given are for ^adaytime, ^bthe cities of Florence (Matese et al., 2009) and Łódź (Fortuniak et al., 2013), and ^cthe municipality of Beijing (Liu et al., 2012).

Site	F_C [kg C m ⁻² yr ⁻¹]	P_V [%]	ρ_{pop} [km ⁻²]	Observation period	Reference
London	12.72	5	^a 31,000	2011–2012	This study
London (He11)	9.67	8	^a 22,500	Oct 2006–May 2008	Helfter et al. (2011)
Florence (Gi12)	8.27	≈ 2	^b 3470	Mar 2005–Jun 2011	Gioli et al. (2012)
Vancouver (Ch11)	6.71	35	6420	May 2008–Apr 2010	Christen et al. (2011)
Montreal URB (BS11)	5.56	29	8400	Nov 2007–Sep 2009	Bergeron and Strachan (2011)
Beijing (Li12)	4.90	≈ 15	^c 1309	2006–2009	Liu et al. (2012)
Tokyo (MK04)	3.35	21	11,800	May 2001–Apr 2002	Moriwaki and Kanda (2004)
Łódź (Pa10)	2.95	38	^b 9375	Jul 2006–Aug 2008	Pawlak et al. (2010)
Melbourne (Co07)	2.32	38	2939	Feb 2004–Jun 2005	Coutts et al. (2007)
Singapore (Ve13)	1.77	15	7491	Oct 2010–Jun 2012	Velasco et al. (2013)
Helsinki (Ja12)	1.76	44	3262	2006–2010	Järvi et al. (2012)
Swindon	1.75	44	4700	2011–2012	This study
Montreal SUB (BS11)	1.42	50	3150	Nov 2007–Sep 2009	Bergeron and Strachan (2011)
Baltimore (Cr11)	0.36	67	1500	2002–2006	Crawford et al. (2011)

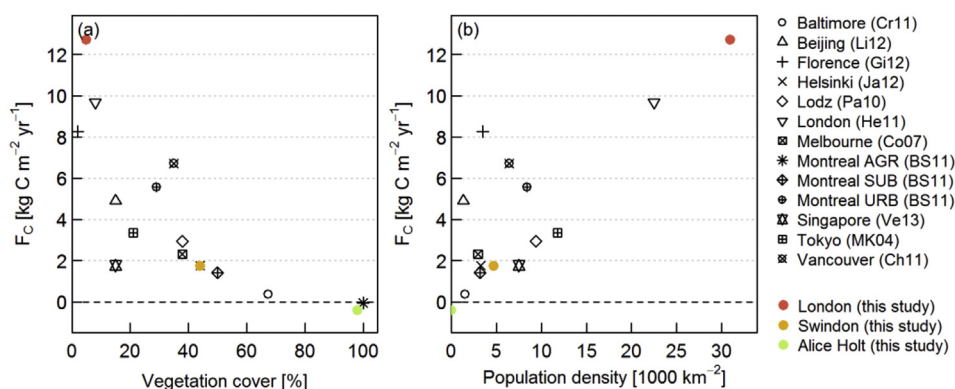


Fig. 12. Annual net carbon exchange for the three sites in this study (London (urban), Swindon (suburban) and Alice Holt (woodland)) versus (a) plan area vegetation cover and (b) population density, alongside values from the literature (see Table 3 for references).

given for the London studies in Table 3 and Fig. 12b; resident population densities would be much smaller and total daytime population densities including tourists would be much higher (Section 4.2.3). The population estimate given in Liu et al. (2012) is for the whole Beijing municipality and is very low for the compact, built-up nature of their study site; 10,000–20,000 persons km^{-2} seems more appropriate for the measurement footprint. Similarly, 3470 persons km^{-2} (Matese et al., 2009) is a very low estimate for the particular area around the central Florence site which has a 'very high population density', as discussed in Gioli et al. (2012). Such variation in population density therefore limits its usefulness as an estimator for F_C .

The distribution of points in Fig. 12b highlights the need for more observations in very densely urbanised areas. The two studies with the largest fluxes and highest population densities took place in London. The central London annual carbon release measured in this study is the largest to date, corresponding to the site with the highest population density and low vegetation cover. The second largest emissions are also from London, and are associated with a slightly higher vegetation fraction and slightly lower population density (Helfter et al., 2011). These measurements were made at a height of 190 m and so had a much larger footprint than the present study. Highly-vegetated low-density suburban Baltimore has the smallest F_C of the urban sites of $0.361 \text{ kg C m}^{-2} \text{ yr}^{-1}$ (Crawford et al., 2011).

Given the diversity of sites in Fig. 12, the vegetation fraction is a useful proxy for approximating carbon emissions from urban areas. Besides the plan area of vegetation cover, species and biomass may also be relevant (Velasco et al., 2013), for example evergreens have greater potential for carbon assimilation compared with deciduous trees (Falge et al., 2002). Variation in net ecosystem exchange among vegetated ecosystems is about $1 \text{ kg C m}^{-2} \text{ yr}^{-1}$, ranging from small CO_2 release to CO_2 uptake approaching $-0.9 \text{ kg C m}^{-2} \text{ yr}^{-1}$ (Falge et al., 2002; Soussana et al., 2007; Thomas et al., 2011; Wilkinson et al., 2012). This variation, however, is only about 10% of the variation in studied urban sites ($>12 \text{ kg C m}^{-2} \text{ yr}^{-1}$). Some studies have suggested that urbanisation reduces natural variability and has a homogenising effect on ecology as a result of similar land use, land management and species selection across the globe (McKinney, 2006; Groffman et al., 2014; Polsky et al., 2014).

Some of the spread within Fig. 12 can be attributed to climatic differences, for example emissions in urban Montreal are relatively high given the vegetation fraction of the site due to fossil fuel combustion for building heating (Bergeron and Strachan, 2011), whilst the year-round warm climate in Singapore means emissions from buildings are limited to combustion for cooking (Velasco et al.,

2013). The net exchange for the Swindon, Helsinki and Singapore sites are almost identical (Table 3). Swindon and Helsinki have broadly similar climates, the same amount of vegetation cover ($P_V = 44\%$) and similar population densities, whilst the effects of Singapore's tropical climate with no heating requirement balances the smaller proportion of vegetation ($P_V = 15\%$) and higher population density. Contrary to findings elsewhere, summertime carbon release in semi-arid Salt Lake Valley was smaller for a highly-vegetated suburban site ($P_V = 49\%$) compared to the surrounding natural grasslands, partially attributed to the dormancy of the grasslands during dry conditions compared to irrigated suburban vegetation and abundance of non-native trees in the suburban area (Ramamurthy and Pardyjak, 2011).

Compared with the differences between sites, variation between measurement years is small. In Beijing, F_C was found to be closely related to traffic load, ranging from 4.61 to $5.40 \text{ kg C m}^{-2} \text{ yr}^{-1}$ (2006–2009). Traffic restrictions during the 2008 Olympic Games reduced the number of vehicles by 60% and coincided with the lowest annual emissions (Liu et al., 2012). These traffic restrictions were estimated to reduce daily carbon fluxes by about 30% (Song and Wang, 2012). In Helsinki, observed F_C ranges from 1.58 to $1.88 \text{ kg C m}^{-2} \text{ yr}^{-1}$ (2006–2010), with inter-annual variability attributed to synoptic weather conditions (both the exceptionally warm and sunny conditions in summer 2006 and the influence of wind direction on flux footprint) (Järvi et al., 2012).

Differences in F_C between sites can occur due to footprint composition, particularly when strong localised sources such as industry or roads are located nearby. Annual flux estimates over a suburban lawn (Hiller et al., 2011) were adjusted by $0.13 \text{ kg C m}^{-2} \text{ yr}^{-1}$ to account for the impact of a nearby road (carrying approx. 10,000 vehicles day^{-1}), hence even a small area of road (small change in P_V) can lead to appreciable differences in annual CO_2 exchange. The higher-than-expected net exchange for Vancouver given the vegetation cover and population density (Fig. 12) is attributed to the proximity of major roads to the measurement tower (Christen et al., 2011). Urban sites generally consist of a complex spatial distribution of sources and sinks of CO_2 . Whilst the woodland site is fairly homogeneous, in Swindon larger CO_2 release is observed from the area south-west of the tower where there is a busy crossroads and greater CO_2 uptake is seen to the north-east when the source area contains more gardens and large trees. Differences in CO_2 exchange between 90° sectors due to local heterogeneity may be about $0.6 \text{ kg C m}^{-2} \text{ yr}^{-1}$ at S, which is of a similar magnitude as would be expected from Fig. 12 for a change in P_V of $\approx 10\%$. The prevailing wind direction at S is south-westerly, hence F_C is expected to be biased to higher values compared with

the study area as a whole (Ward et al., 2013). In London, F_C tends to be higher when the source area includes a busy junction to the north and smaller when the source area includes the River Thames to the south (see Kotthaus and Grimmond, 2014b for analysis of the spatial variability in energy fluxes at the central London site). Measurements of CO_2 concentration within streets indicate higher variability close to the river, where the air is generally cleaner but CO_2 'hotspots' occur in areas of high traffic load, however, there is little spatial variation in concentrations for roads that are not adjacent to the river. Differences in F_C related to land cover variation at each site individually are far smaller than the differences between sites.

5. Conclusions

In this paper, we examine direct observations of the carbon dioxide exchange from three very different sites in close proximity monitored over the same multi-seasonal time period: a woodland site at Alice Holt, a suburban site in Swindon and a dense urban site in central London. These sites are subject to the same meteorological conditions, and thus related drivers have little effect on the observed differences (as they are effectively constant across the sites). Differences in the exchange of CO_2 between surface and atmosphere can therefore be attributed to processes related to land use. Comparison of three sites of different land cover is useful because trends begin to form when the sites are ranked by urban density. The results shown here support previous findings on the relation between CO_2 fluxes and building fraction (or the close to inverse relation with vegetation fraction), as shown in Grimmond and Christen (2012), Nordbo et al. (2012) or Weissert et al. (2014) for example. The huge anthropogenic emissions associated with cities means that variation in annual CO_2 exchange among urbanised study sites is about ten times that observed among vegetated ecosystems.

Signatures of different anthropogenic and biogenic controls were investigated at various timescales. At sites with a significant proportion of (deciduous) vegetation, fluxes are very different between the summer growing season and winter. Photosynthetic uptake dominates the diurnal and seasonal cycle at the forested Alice Holt site, but also plays a key role in the carbon cycle of suburban Swindon (44% vegetated), where daily summertime net carbon emissions are small. That photosynthesis is an important component of the total measured flux is illustrated by tight F_C -PAR curves exhibited by the suburban and woodland data. Net CO_2 uptake is not seen in central London. Here, the times of smallest CO_2 release are summer night times, coinciding with minimal human activity. Nocturnal emissions are largest during winter for sites where building heating is important, whilst at the woodland site nocturnal emissions peak in summer when warm temperatures and photosynthetic uptake during the day promote respiration.

Total observed carbon exchange for the London site is similar to NAEI values, whilst at Swindon and Alice Holt vegetative and biogenic processes (not included in the NAEI data) play a significant role in the carbon balance. For the urban and suburban site, anthropogenic emissions were modelled at finer time resolution using the GreaterQF model and statistics of energy and vehicle use respectively. Comparison with the observed fluxes suggests the anthropogenic emissions are overestimated by this approach for Swindon, while estimates for London are highly dependent on the spatial resolution of the inventory data. However the models effectively replicate the impact of patterns in human behaviour on carbon exchange. Validation of the inventory approach to estimating emissions at smaller scales in heterogeneous environments would require consumption data at higher resolution than currently available and an experimental design whereby the spatial

extent of the inventory and observational data could be well matched.

Urban and suburban patterns of CO_2 fluxes at the sub-daily, weekly and seasonal cycles can be directly attributed to patterns in human behaviour. Traffic and building energy use at both sites closely resemble the single- and double-peaked diurnal cycles observed in F_C in London and Swindon, respectively, and largely explain reduced emissions on weekends compared to weekdays. The major difference between CO_2 release on working days and non-working days illustrates the potential impact that reducing anthropogenic activities (or cutting emissions by improving efficiency) could have. Reductions in traffic intensity, improved energy efficiency in buildings, and preferential use of electricity over combustion of fossil fuels could make a significant impact in limiting carbon release from towns and cities.

The main result of this study is the order of magnitude differences in the net CO_2 exchange at the three very different sites, based on direct contemporaneous observations. It has been shown that the diurnal and seasonal behaviour varies significantly with urban density. At annual timescales, these results provide an independent evaluation of inventory-based assessments. These findings demonstrate, and begin to quantify, the major role urban areas have in global CO_2 emissions.

Acknowledgements

Collection of the datasets used in this study was funded by: EUFP7 Grant BRIDGE (211345), NERC ClearfLo (H003231/1), EPSRC Materials Innovation Hub (EP/I00159X/1, EP/I00159X/2) and King's College London (London); the Natural Environment Research Council, UK (Swindon); the Forestry Commission (Alice Holt). Please contact the authors for further information about the datasets used. We thank Dr Arnold Moene at Wageningen University for providing the ECPack software and for all advice regarding its usage; Dr Jiangping He for support of the London data archive; all staff and students at KCL who contributed to the data collection; KCL Directorate of Estates and Facilities for giving us the opportunity to operate the various measurement sites; and the residents of Swindon who kindly allowed us to install the flux mast in their garden. Finally, we thank the reviewer for their helpful comments.

References

- Aubinet, M., Vesala, T., Papale, D., 2012. Eddy Covariance: a Practical Guide to Measurement and Data Analysis. In: Springer Atmospheric Sciences, p. 438.
- Baldocchi, D., Falge, E., Gu, L., Olson, R., Hollinger, D., Running, S., Anthoni, P., Bernhofer, C., Davis, K., Evans, R., Fuentes, J., Goldstein, A., Katul, G., Law, B., Lee, X., Malhi, Y., Meyers, T., Munger, W., Oechel, W., Paw, K.T., Pilegaard, K., Schmid, H.P., Valentini, R., Verma, S., Vesala, T., Wilson, K., Wofsy, S., 2001. FLUXNET: a new tool to study the temporal and spatial variability of ecosystem-scale carbon dioxide, water vapor, and energy flux densities. *Bull. Am. Meteorol. Soc.* 82, 2415–2434. [http://dx.doi.org/10.1175/1520-0477\(2001\)082<2415:FANTTS>2.3.CO;2](http://dx.doi.org/10.1175/1520-0477(2001)082<2415:FANTTS>2.3.CO;2).
- Baldocchi, D.D., Black, T., Curtis, P., Falge, E., Fuentes, J., Granier, A., Gu, L., Knohl, A., Pilegaard, K., Schmid, H., 2005. Predicting the onset of net carbon uptake by deciduous forests with soil temperature and climate data: a synthesis of FLUXNET data. *Int. J. Biometeorol.* 49, 377–387.
- Bergeron, O., Strachan, I.B., 2011. CO_2 sources and sinks in urban and suburban areas of a northern mid-latitude city. *Atmos. Environ.* 45, 1564–1573.
- Briber, B.M., Hutrya, L.R., Dunn, A.L., Raciti, S.M., Munger, J.W., 2013. Variations in atmospheric CO_2 mixing ratios across a Boston, MA urban to rural gradient. *Land* 2, 304–327.
- Christen, A., 2014. Atmospheric measurement techniques to quantify greenhouse gas emissions from cities. *Urban Clim.* <http://dx.doi.org/10.1016/j.uclim.2014.04.006>.
- Christen, A., Coops, N., Crawford, B., Kellett, R., Liss, K., Olchovski, I., Tooke, T., Van Der Laan, M., Voegt, J., 2011. Validation of modeled carbon-dioxide emissions from an urban neighborhood with direct eddy-covariance measurements. *Atmos. Environ.* 45, 6057–6069.
- Christen, A., Vogt, R., 2004. Energy and radiation balance of a central European city. *Int. J. Climatol.* 24, 1395–1421. <http://dx.doi.org/10.1002/joc.1074>.

- Coutts, A.M., Beringer, J., Tapper, N.J., 2007. Characteristics influencing the variability of urban CO₂ fluxes in Melbourne, Australia. *Atmos. Environ.* 41, 51–62.
- Crawford, B., Christen, A., 2012. Quantifying the CO₂ storage flux term in urban eddy-covariance observations. In: 8th International Conference on Urban Climate, Dublin, Ireland, 6–10 August 2012.
- Crawford, B., Christen, A., 2014. Spatial source attribution of measured urban eddy covariance CO₂ fluxes. *Theor. Appl. Climatol.* 1–23. <http://dx.doi.org/10.1007/s00704-014-1124-0>.
- Crawford, B., Grimmond, C.S.B., Christen, A., 2011. Five years of carbon dioxide fluxes measurements in a highly vegetated suburban area. *Atmos. Environ.* 45, 896–905.
- DECC, 2013a. Department of Energy & Climate Change – Sub-national Electricity and Gas Consumption Statistics: Analysis Tool 2005 to 2012. Retrieved 17 May 2014, from www.gov.uk/government/collections/sub-national-gas-consumption-data.
- DECC, 2013b. Department of Energy & Climate Change: Local and Regional CO₂ Emissions Estimates for 2005–2011. Retrieved 20 May 2014, from www.gov.uk/government/organisations/departement-of-energy-climate-change/series/sub-national-greenhouse-gas-emissions-statistics.
- DfT, 2011. Department for Transport: National Travel Survey 2010 from www.dft.gov.uk/statistics/releases/national-travel-survey-2010.
- DfT, 2013. Department for Transport: Road Traffic Statistics from www.dft.gov.uk/statistics/series/traffic.
- Falge, E., Baldocchi, D., Tenhunen, J., Aubinet, M., Bakwin, P., Berbigier, P., Bernhofer, C., Burba, G., Clement, R., Davis, K.J., 2002. Seasonality of ecosystem respiration and gross primary production as derived from FLUXNET measurements. *Agric. For. Meteorol.* 113, 53–74.
- Flanagan, L.B., Wever, L.A., Carlson, P.J., 2002. Seasonal and interannual variation in carbon dioxide exchange and carbon balance in a northern temperate grassland. *Glob. Change Biol.* 8, 599–615. <http://dx.doi.org/10.1046/j.1365-2486.2002.00491.x>.
- Fortuniak, K., Pawlak, W., Siedlecki, M., 2013. Integral turbulence statistics over a Central European city Centre. *Bound. Layer Meteorol.* 146, 257–276. <http://dx.doi.org/10.1007/s10546-012-9762-1>.
- Gioli, B., Toscano, P., Lugato, E., Matese, A., Miglietta, F., Zaldei, A., Vaccari, F., 2012. Methane and carbon dioxide fluxes and source partitioning in urban areas: the case study of Florence, Italy. *Environ. Pollut.* 164, 125–131.
- GLA, 2013. Daytime Population, Borough. Retrieved 10 Oct 2014, from data.london.gov.uk/datastore/package/daytime-population-borough.
- Grimmond, C.S.B., Christen, A., 2012. Flux measurements in urban ecosystems. *FluxLetter* 5, 1–8.
- Grimmond, C.S.B., King, T.S., Cropley, F.D., Nowak, D.J., Souch, C., 2002. Local-scale fluxes of carbon dioxide in urban environments: methodological challenges and results from Chicago. *Environ. Pollut.* 116, S243–S254.
- Grimmond, C.S.B., Salmond, J.A., Oke, T.R., Offerle, B., Lemonsu, A., 2004. Flux and turbulence measurements at a densely built-up site in Marseille: heat, mass (water and carbon dioxide), and momentum. *J. Geophys. Res. (Atmos.)* 109, D24101. <http://dx.doi.org/10.1029/2004jd004936>.
- Groffman, P.M., Cavender-Bares, J., Bettez, N.D., Grove, J.M., Hall, S.J., Heffernan, J.B., Hobbie, S.E., Larson, K.L., Morse, J.L., Neill, C., Nelson, K., O'Neil-Dunne, J., Ogden, L., Pataki, D.E., Polsky, C., Chowdhury, R.R., Steele, M.K., 2014. Ecological homogenization of urban USA. *Front. Ecol. Environ.* 12, 74–81. <http://dx.doi.org/10.1890/120374>.
- Hamilton, I.G., Davies, M., Steadman, P., Stone, A., Ridley, I., Evans, S., 2009. The significance of the anthropogenic heat emissions of London's buildings: a comparison against captured shortwave solar radiation. *Build. Environ.* 44, 807–817.
- Heinemeyer, A., Wilkinson, M., Vargas, R., Subke, J.A., Casella, E., Morison, J.I.L., Ineson, P., 2012. Exploring the "overflow tap" theory: linking forest soil CO₂ fluxes and individual mycorrhizosphere components to photosynthesis. *Biogeosciences* 9, 79–95. <http://dx.doi.org/10.5194/bg-9-79-2012>.
- Helfter, C., Famulari, D., Phillips, G.J., Barlow, J.F., Wood, C.R., Grimmond, C.S.B., Nemitz, E., 2011. Controls of carbon dioxide concentrations and fluxes above central London. *Atmos. Chem. Phys.* 11, 1913–1928. <http://dx.doi.org/10.5194/acp-11-1913-2011>.
- Hiller, R.V., McFadden, J.P., Kljun, N., 2011. Interpreting CO₂ fluxes over a suburban lawn: the influence of traffic emissions. *Bound. Layer Meteorol.* 138, 215–230. <http://dx.doi.org/10.1007/s10546-010-9558-0>.
- Iamarino, M., Beevers, S., Grimmond, C.S.B., 2012. High-resolution (space, time) anthropogenic heat emissions: London 1970–2025. *Int. J. Climatol.* 32, 1754–1767. <http://dx.doi.org/10.1002/joc.2390>.
- Ichinose, T., Shimodozono, K., Hanaki, K., 1999. Impact of anthropogenic heat on urban climate in Tokyo. *Atmos. Environ.* 33, 3897–3909.
- IEA, 2012. World Energy Outlook 2012, p. 700.
- Imhoff, M.L., Bounoua, L., DeFries, R., Lawrence, W.T., Stutzer, D., Tucker, C.J., Ricketts, T., 2004. The consequences of urban land transformation on net primary productivity in the United States. *Remote Sens. Environ.* 89, 434–443. <http://dx.doi.org/10.1016/j.rse.2003.10.015>.
- Järvi, L., Nordbo, A., Junninen, H., Riikonen, A., Moilanen, J., Nikinmaa, E., Vesala, T., 2012. Seasonal and annual variation of carbon dioxide surface fluxes in Helsinki, Finland, in 2006–2010. *Atmos. Chem. Phys.* 12, 8475–8489. <http://dx.doi.org/10.5194/acp-12-8475-2012>.
- Koerner, B., Klopatek, J., 2002. Anthropogenic and natural CO₂ emission sources in an arid urban environment. *Environ. Pollut.* 116, S45–S51.
- Kotthaus, S., Grimmond, C.S.B., 2012. Identification of micro-scale anthropogenic CO₂, heat and moisture sources – processing eddy covariance fluxes for a dense urban environment. *Atmos. Environ.* 57, 301–316.
- Kotthaus, S., Grimmond, C.S.B., 2014a. Energy exchange in a dense urban environment – Part I: temporal variability of long-term observations in central London. *Urban Clim.* <http://dx.doi.org/10.1016/j.uclim.2013.10.002>.
- Kotthaus, S., Grimmond, C.S.B., 2014b. Energy exchange in a dense urban environment – Part II: impact of spatial heterogeneity of the surface. *Urban Clim.* <http://dx.doi.org/10.1016/j.uclim.2013.10.001>.
- Lietzke, B., Vogt, R., 2013. Variability of CO₂ concentrations and fluxes in and above an urban street canyon. *Atmos. Environ.* 74, 60–72.
- Liu, H., Feng, J., Järvi, L., Vesala, T., 2012. Four-year (2006–2009) eddy covariance measurements of CO₂ flux over an urban area in Beijing. *Atmos. Chem. Phys.* 12, 7881–7892.
- Lloyd, J., Taylor, J., 1994. On the temperature dependence of soil respiration. *Funct. Ecol.* 315–323.
- Matese, A., Gioli, B., Vaccari, F.P., Zaldei, A., Miglietta, F., 2009. Carbon dioxide emissions of the City Center of Firenze, Italy: measurement, evaluation, and source partitioning. *J. Appl. Meteorol. Climatol.* 48, 1940–1947. <http://dx.doi.org/10.1175/2009jamc1945.1>.
- McKinney, M.L., 2006. Urbanization as a major cause of biotic homogenization. *Biol. Conserv.* 127, 247–260. <http://dx.doi.org/10.1016/j.biocon.2005.09.005>.
- Met Office, 2014a. Mean Temperature. Retrieved 31/03/2014, from metoffice.gov.uk/pub/data/weather/uk/climate/datasets/Tmean/date/England_SE_and_Central_S.txt.
- Met Office, 2014b. Rainfall. Retrieved 31/03/2014, from metoffice.gov.uk/pub/data/weather/uk/climate/datasets/Rainfall/date/England_SE_and_Central_S.txt.
- Mizunuma, T., Wilkinson, M., Eaton, L.E., Mencuccini, M., Morison, J.I.L., Grace, J., 2013. The relationship between carbon dioxide uptake and canopy colour from two camera systems in a deciduous forest in southern England. *Funct. Ecol.* 27, 196–207. <http://dx.doi.org/10.1111/1365-2435.12026>.
- Moriwaki, R., Kanda, M., 2004. Seasonal and diurnal fluxes of radiation, heat, water vapor, and carbon dioxide over a suburban area. *J. Appl. Meteorol.* 43, 1700–1710.
- NAEI, 2011. National Atmospheric Emissions Inventory. Retrieved 14 May 2014, from naei.defra.gov.uk/data/gis-mapping.
- Nemitz, E., Hargreaves, K.J., McDonald, A.G., Dorsey, J.R., Fowler, D., 2002. Meteorological measurements of the urban heat budget and CO₂ emissions on a city scale. *Environ. Sci. Technol.* 36, 3139–3146. <http://dx.doi.org/10.1021/es10277e>.
- NGVA, "Comparison of energy contents and CO₂ emissions from different fuels." Retrieved 17 May 2014, from www.ngvaeurope.eu/comparison-of-energy-contents-and-co2-emissions-from-different-fuels.
- Nordbo, A., Järvi, L., Haapanala, S., Wood, C.R., Vesala, T., 2012. Fraction of natural area as main predictor of net CO₂ emissions from cities. *Geophys. Res. Lett.* 39, L20802. <http://dx.doi.org/10.1029/2012GL053087>.
- Oke, T.R., Crowther, J.M., McNaughton, K.G., Monteith, J.L., Gardiner, B., 1989. The Micrometeorology of the urban Forest (and discussion). *Philos. Trans. R. Soc. Lond. B Biol. Sci.* 324, 335–349. <http://dx.doi.org/10.1098/rstb.1989.0051>.
- ONS, 2011. Office for National Statistics – Census 2011. Retrieved 17 May 2014, from www.nomisweb.co.uk/census/2011.
- Papale, D., Reichstein, M., Aubinet, M., Canfora, E., Bernhofer, C., Kutsch, W., Longdoz, B., Rambal, S., Valentini, R., Vesala, T., Yakir, D., 2006. Towards a standardized processing of Net Ecosystem Exchange measured with eddy covariance technique: algorithms and uncertainty estimation. *Biogeosciences* 3, 571–583. <http://dx.doi.org/10.5194/bg-3-571-2006>.
- Pataki, D.E., Carreiro, M.M., Cherrier, J., Grulke, N.E., Jennings, V., Pincetl, S., Pouyat, R.V., Whitlow, T.H., Zipperer, W.C., 2011. Coupling biogeochemical cycles in urban environments: ecosystem services, green solutions, and misconceptions. *Front. Ecol. Environ.* 9, 27–36. <http://dx.doi.org/10.1890/090220>.
- Pawlak, W., Fortuniak, K., Siedlecki, M., 2010. Carbon dioxide flux in the centre of Łódź, Poland – analysis of a 2-year eddy covariance measurement data set. *Int. J. Climatol.* 31, 232–243. <http://dx.doi.org/10.1002/joc.2247>.
- Peixoto, J.P., Oort, A.H., 1992. *Physics of Climate*. American Institute of Physics, p. 520.
- Perpiñán, O., 2012. solaR: solar radiation and photovoltaic systems with R. *J. Stat. Softw.* 50, 1–32.
- Peters, E.B., McFadden, J.P., 2012. Continuous measurements of net CO₂ exchange by vegetation and soils in a suburban landscape. *J. Geophys. Res. Biogeosci.* (2005–2012) 117.
- Polksy, C., Grove, J.M., Knudson, C., Groffman, P.M., Bettez, N., Cavender-Bares, J., Hall, S.J., Heffernan, J.B., Hobbie, S.E., Larson, K.L., Morse, J.L., Neill, C., Nelson, K.C., Ogden, L.A., O'Neil-Dunne, J., Pataki, D.E., Roy Chowdhury, R., Steele, M.K., 2014. Assessing the homogenization of urban land management with an application to US residential lawn care. *Proc. Natl. Acad. Sci.* 111, 4432–4437. <http://dx.doi.org/10.1073/pnas.1323995111>.
- Ramamurthy, P., Pardyjak, E.R., 2011. Toward understanding the behavior of carbon dioxide and surface energy fluxes in the urbanized semi-arid Salt Lake Valley, Utah, USA. *Atmos. Environ.* 45, 73–84. <http://dx.doi.org/10.1016/j.jatmosenv.2010.09.049>.
- Ryder, C.L., Toomi, R., 2011. An urban solar flux island: measurements from London. *Atmos. Environ.* 45, 3414–3423. <http://dx.doi.org/10.1016/j.jatmosenv.2011.03.045>.
- Sailor, D.J., 2011. A review of methods for estimating anthropogenic heat and moisture emissions in the urban environment. *Int. J. Climatol.* 31, 189–199. <http://dx.doi.org/10.1002/joc.2106>.

- Sailor, D.J., Lu, L., 2004. A top-down methodology for developing diurnal and seasonal anthropogenic heating profiles for urban areas. *Atmos. Environ.* 38, 2737–2748.
- Schmid, H.P., Grimmer, C.S.B., Cropley, F., Offerle, B., Su, H.-B., 2000. Measurements of CO₂ and energy fluxes over a mixed hardwood forest in the mid-western United States. *Agric. For. Meteorol.* 103, 357–374.
- Seto, K.C., Shepherd, J.M., 2009. Global urban land-use trends and climate impacts. *Curr. Opin. Environ. Sustain.* 1, 89–95. <http://dx.doi.org/10.1016/j.cosust.2009.07.012>.
- Song, T., Wang, Y., 2012. Carbon dioxide fluxes from an urban area in Beijing. *Atmos. Res.* 106, 139–149.
- Soussana, J.F., Allard, V., Pilegaard, K., Ambus, P., Amman, C., Campbell, C., Ceschia, E., Clifton-Brown, J., Czobel, S., Domingues, R., Flechard, C., Fuhrer, J., Hensen, A., Horvath, L., Jones, M., Kasper, G., Martin, C., Nagy, Z., Neftel, A., Raschi, A., Baronti, S., Rees, R.M., Skiba, U., Stefani, P., Manca, G., Sutton, M., Tuba, Z., Valentini, R., 2007. Full accounting of the greenhouse gas (CO₂, N₂O, CH₄) budget of nine European grassland sites. *Agric. Ecosyst. Environ.* 121, 121–134. <http://dx.doi.org/10.1016/j.agee.2006.12.022>.
- Strong, C., Stwertka, C., Bowling, D.R., Stephens, B.B., Ehleringer, J.R., 2011. Urban carbon dioxide cycles within the Salt Lake Valley: a multiple-box model validated by observations. *J. Geophys. Res. (Atmos)* 116, D15307. <http://dx.doi.org/10.1029/2011JD015693>.
- TfL, 2012. London 2012 Games Transport – Performance, Funding and Legacy. Retrieved 12 May 2014, from. www.tfl.gov.uk/cdn/static/cms/documents/Part-1-Item06-TfL-Games-performance-Final-corrected.pdf.
- The Keeling Curve, 2014. Retrieved 31/03/2014, from. keelingcurve.ucsd.edu/.
- Thomas, M.V., Malhi, Y., Fenn, K.M., Fisher, J.B., Morecroft, M.D., Lloyd, C.R., Taylor, M.E., McNeil, D.D., 2011. Carbon dioxide fluxes over an ancient broad-leaved deciduous woodland in southern England. *Biogeosciences* 8, 1595–1613. <http://dx.doi.org/10.5194/bg-8-1595-2011>.
- van Dijk, A., Moene, A.F., de Bruin, H.A.R., 2004. *The Principles of Surface Flux Physics: Theory, Practice and Description of the ECPACK Library*, p. 99.
- Velasco, E., Roth, M., 2010. Cities as net sources of CO₂: review of atmospheric CO₂ exchange in urban environments measured by eddy covariance technique. *Geogr. Compass* 4, 1238–1259. <http://dx.doi.org/10.1111/j.1749-8198.2010.00384.x>.
- Velasco, E., Roth, M., Tan, S.H., Quak, M., Nabarro, S.D.A., Norford, L., 2013. The role of vegetation in the CO₂ flux from a tropical urban neighbourhood. *Atmos. Chem. Phys.* 13, 10185–10202. <http://dx.doi.org/10.5194/acp-13-10185-2013>.
- Ward, H.C., Evans, J.G., Grimmer, C.S.B., 2013. Multi-season eddy covariance observations of energy, water and carbon fluxes over a suburban area in Swindon, UK. *Atmos. Chem. Phys.* 13, 4645–4666. <http://dx.doi.org/10.5194/acp-13-4645-2013>.
- Weissert, L.F., Salmond, J.A., Schwendenmann, L., 2014. A review of the current progress in quantifying the potential of urban forests to mitigate urban CO₂ emissions. *Urban Clim.* <http://dx.doi.org/10.1016/j.uclim.2014.01.00>.
- Wilkinson, M., Eaton, E.L., Broadmeadow, M.S.J., Morison, J.I.L., 2012. Inter-annual variation of carbon uptake by a plantation oak woodland in south-eastern England. *Biogeosciences* 9, 5373–5389. <http://dx.doi.org/10.5194/bg-9-5373-2012>.
- Zhang, X., Friedl, M.A., Schaaf, C.B., Strahler, A.H., Schneider, A., 2004. The footprint of urban climates on vegetation phenology. *Geophys. Res. Lett.* 31, L12209. <http://dx.doi.org/10.1029/2004gl020137>.